

Available online at <http://www.mecspress.net/ijwmt>

# Interference Mitigation Techniques for Spectral Capacity Enhancement in GSM Networks

Ahmed M. Alaa<sup>a</sup>, Hazim Tawfik<sup>b</sup>

<sup>a,b</sup> *Design Laboratory for Electronics and Communication Systems (DLECS), Faculty of Engineering, Cairo University, Gizah, Egypt*

---

## Abstract

Random Frequency Hopping (FH) is a key feature of GSM networks that allows for capacity enhancement. The increased co-channel interference experienced in networks with tight frequency reuse schemes can be mitigated by adopting frequency hopping. Frequency hopping diversifies the interference signals over sparse transmitted bursts. This effect is called Interference Diversity. Interference Diversity allows the Forward Error Correcting codes (FEC) to easily correct the corrupted bits. Thus, frequency hopping allows the network operator to use a tighter frequency reuse scheme without exhibiting higher levels of co-channel interference.

Discontinuous Transmission (DTX) is another interference mitigation method that utilizes the user's silence frames to reduce the transmitted power, while Power Control (PC) links the transmitted handset power with its relative distance from the Base Station (BTS). In this work, we study the impact of random FH, DTX and PC on the Spectral Capacity of GSM cellular networks by means of combined link level and system level simulation. It is shown that a spectral capacity gain is obtained in a 3/9 reuse scheme that deploys PC, DTX and FH compared to a conventional 4/12 reuse scheme.

**Index Terms:** Random Frequency Hopping (FH), Power Control (PC), Discontinuous Transmission (DTX), Interference Diversity, Frequency diversity, Spectral Capacity.

© 2014 Published by MECS Publisher. Selection and/or peer review under responsibility of the Research Association of Modern Education and Computer Science

---

## 1. Introduction

The increasing number of subscribers imposes capacity constraints on network operators due to the limited spectrum assigned to each operator. Techniques for capacity enhancement are adopted by operators to meet the increasing capacity demand. Increasing the system capacity can be achieved by adopting a lower reuse scheme. The implication of decreasing the reuse figure is increasing co-channel interference and thus, the quality degrades. Techniques for increasing the interference immunity will consequently increase the capacity as we can adopt a lower reuse figure without sacrificing the Quality of Service (QoS). Those techniques include:

\* Corresponding author. Tel.: 86 18796022027; fax: 86 511 88791128  
E-mail address: zhuzhipan888@163.com

Discontinuous Transmission (DTX), Power Control (PC) and Frequency Hopping (FH). Frequency hopping is a process of changing the RF carrier frequency in a prescribed rate. There are two classes of frequency hopping according to the hopping rate: Slow FH and Fast FH. Slow frequency hopping refers to changing the RF carrier for every new burst, while fast FH refers to changing the RF carrier in a rate higher than the modulation rate. Frequency hopping is also classified based on frequency selection approach into: Random FH and Cyclic FH. The cyclic hopping follows a pre-defined list of frequencies in a regular order, while random hopping transceivers selects a frequency randomly out of a predefined list. FH transceivers are also classified based on their implementation: Baseband FH (BH) requires a dedicated transceiver for each RF carrier within the hopping sequence, while Synthesizer FH (SH) relies on tuning the transceiver on a specific carrier frequency (this requires wideband RF equipment). In this work, we consider slow frequency hopping with random, baseband hopping frequency generation for GSM transmission.

The bursts within a TDMA (Time Division Multiple Access) frame are subjected to different values of co-channel interference because hopping causes different signals to interfere with carrier signal at different times. This effect is called interference diversity. On a system level, the effective interference between users is reduced; this effect is called interference averaging. In addition to the Interference diversity effect, frequency hopping results in a Frequency diversity effect; the frequency selective fading pattern is changed due to the change of the RF carrier. Hence, consecutive bursts are less probable to be subjected to fading dips.

The QoS criterion for systems with random frequency hopping is based on thresholds of Bit Error Rate (BER) or Frame Error Rate (FER). This means that we need to map the Carrier-to-Interference ratio ( $C/I$ ) values on different bursts to corresponding FERs/BERs. To accomplish this, we have to integrate a link level model with a system model. The  $C/I$  values obtained from the system model are fed into the link model to obtain error rate estimates. The goal of this work is to study how the incorporated interference mitigation techniques can allow the network operator to adopt a tighter frequency reuse scheme, increasing the network's overall capacity. The paper is divided as follows. Section II presents the GSM system level model, the simulation methodology and the  $C/I$  statistical results for the system with Power Control (PC) and Discontinuous Transmission (DTX) features enabled. Section III discusses frequency hopping and the concepts behind it, and presents the link level model used for mapping  $C/I$  ratios to FER/BER based on the GSM physical layer. Section IV shows the adopted propagation and channel models used in the simulation. Finally, simulation results for FER and BER CDF are presented and the spectral capacity gain due to interference diversity is shown for a simulation environment that accounts for all practical considerations.

## 2. System Model

The basic system level simulation considers the first tier of co-channel interferers only. Thus, for all reuse schemes, the number of interferers is limited to 6. Figure 1 shows the home cell and the six reuse cells representing the first tier of interferers. The distance  $R$  denotes the cell radius, while the distance  $D$  denotes the reuse distance.

The Carrier-to-interference ( $C/I$ ) ratio is the performance metric that is used to express the level of co-channel interference. The more the  $C/I$  ratio is, the less co-channel interference we have and there is a room for applying a tighter reuse figure without loss of quality. The  $C/I$  value should not be less than a certain threshold for more than 10% of the service area. This percentage is called the outage probability. The  $C/I$  cumulative density function is used to calculate the  $C/I$  value that is satisfied at 10% of the service area. This value will indicate the interference-wise performance of the network. By adopting different interference mitigation techniques (i.e. PC, FH and DTX), we expect the  $C/I$  ratio that occurs at 10% of the service area will increase.

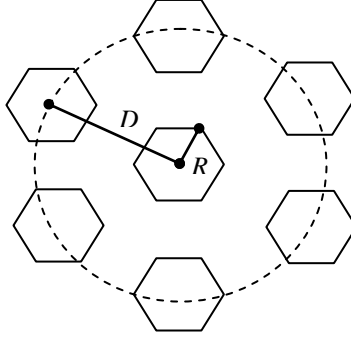


Fig 1 the home cell and reuse cells of the first interferers' tier

Based on a Monte Carlo simulation process, we aim at obtaining the probability and cumulative density functions (PDF and CDF) of the Carrier-to-interference ratio. This is achieved by generating random locations for the Mobile Station (MS) in the home cell based on a uniform PDF, and the same for the six first tier interferers. Assuming a Monte Carlo process with sufficient iterations, the distance between the MS and the Base station (BTS) for the  $i$ th iteration is  $r_i$ , the distance between the  $k$ th interferer and the BTS of the home cell  $d_{ik}$  and the Propagation exponent  $\gamma$ , the C/I ratio in the  $i$ th iteration can be calculated as [1]:

$$\left(\frac{C}{I}\right)_i = \frac{r_i^{-\gamma}}{\sum_{k=1}^6 d_{ik}^{-\gamma}} \quad (1)$$

In the absence of fading and setting  $\gamma = 4$ , the C/I value satisfied at 10% outage is 22 dB. We expect this value to be boosted by adding Power control (PC) and Discontinuous Transmission (DTX) features. If the gain obtained from PC, DTX and FH exceeds the loss of C/I due to decreasing the reuse figure, then we can adopt a lower reuse figure with no loss of transmission quality while maintaining the QoS requirements. Figure 2 shows the PDF of the C/I ratio in a network with a reuse figure  $N = 7$  and path loss exponent  $\gamma = 4$ . Figure 3 shows the CDF of C/I showing that a 22 dB carrier to interference ratio is encountered at 10% of the service area.

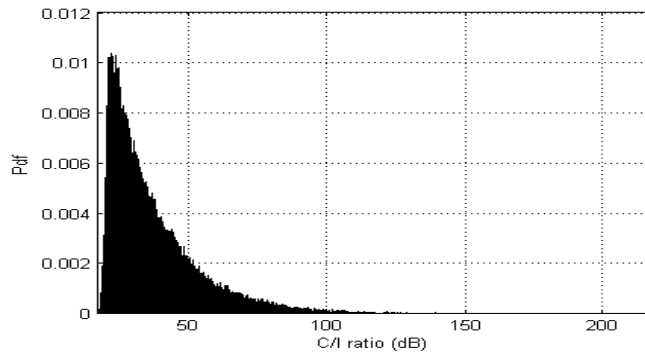


Fig 2 the Carrier-to-Interference ratio probability density function with  $N = 7$  and  $\gamma = 4$

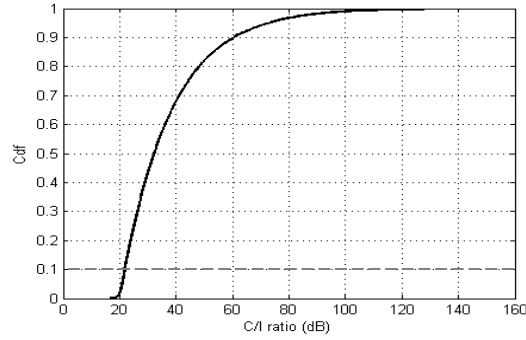


Fig 3 the Carrier-to-Interference ratio cumulative density function with  $N = 7$  and  $\gamma = 4$

### 2.1. Enabling Power Control Feature

Transmit power control algorithms are used to alter the transmit power according to the distance between the Mobile Station (MS) and the Base Station (BTS). If the MS is quite near to the BTS, it can transmit the signal with a lower power level. This will allow reducing the interfering power, and the C/I value with 10% outage is expected to increase significantly. The adopted power control algorithm divides the cell into seven concentric rings. When the MS is located at the farthest ring to the BTS, the transmit power is maximum (no attenuation is applied to the transmit signal). The transition between every two rings results in a power attenuation of 2 dB. When enabling the power control feature in the Monte Carlo simulation process, the cumulative density function of the C/I ratio is shifted to the right and a C/I gain is obtained. The 10% outage probability is satisfied at 25 dB C/I ratio instead of 22 dB in the case when no power control was applied. This means that power control offers 3 dB gain to the C/I quality metric and we have a room for adopting a tighter reuse scheme with the user experiencing no quality loss.

This power control algorithm is depicted mathematically by expressing the attenuation of the transmitted power as a function of the distance between the MS and the BTS. Let the distance between the MS and the BTS be  $d$ , the cell radius  $R$  and the power attenuation per ring is  $M$  dB. The attenuation  $\sigma$  is:

$$\sigma = -M \left( 7 - \text{round} \left( \frac{7d}{R} \right) \right) \quad (2)$$

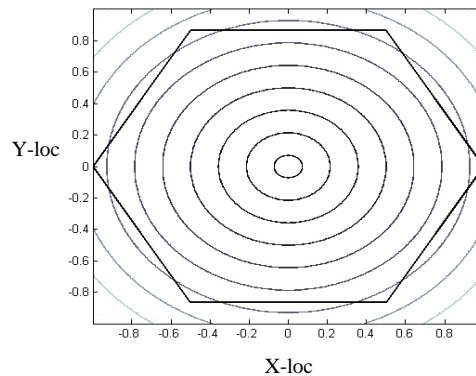


Fig 4 the concentric rings within a hexagonal cell, every new ring results in 2 dB attenuation in the transmitted power

## 2.2. Enabling Discontinuous Transmission (DTX) Feature

Discontinuous Transmission (DTX) is a capacity enhancement technique that exploits the silence speech frames in order to switch off or reduce the transmitted power with a predefined attenuation factor. This feature results in power saving in the MS battery, and either a reduction in the overall interference or an increased capacity by lowering the reuse factor of the network. The percentage of time where the user is talking is called the Voice Activity Factor. From Monte Carlo simulations, it was found that for a 40% activity factor, a gain of 3.4 dB is obtained in the C/I ratio. A 10% outage is satisfied at 25.4 dB Carrier-to-Interference ratio instead of 22 dB. Figure 5 shows the effect of different percentages of the voice activity on the Carrier-to-Interference ratio statistics.

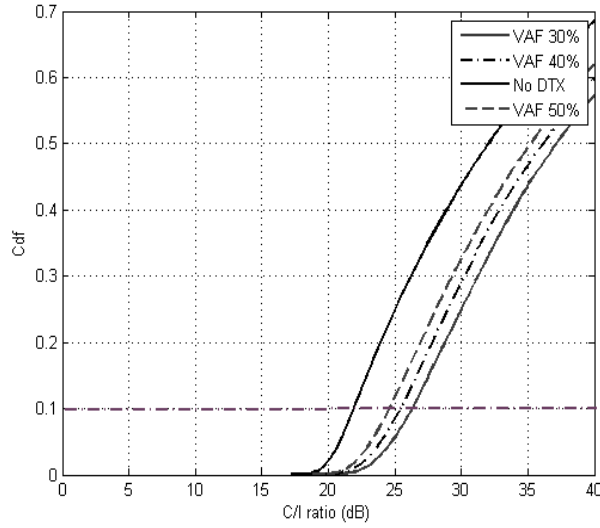


Fig 5 the CDF (Cumulative Density Function) for VAF of 30%, 40% and 50% compared to the case of no DTX

## 2.3. Analytical Framework for exact outage probability calculation

The results of Monte Carlo simulations can be verified by comparing the theoretical worst case Carrier-to-Interference ratio with the C/I ratio with minimum CDF value obtained from simulations. In this section, we verify the results of the Monte Carlo simulation results and propose an analytical framework for calculating the outage probability of the C/I ratio.

According to [1], the worst case interferers' configuration is the one shown in figure 6. By defining the cochannel reuse ratio  $Q = D/R$ , the worst case C/I ratio can be given as:

$$\frac{C}{I} = \frac{R^{-\gamma}}{2(D-R)^{-\gamma} + 2(D+R)^{-\gamma} + 2D^{-\gamma}} = \frac{1}{2(Q-1)^{-\gamma} + 2(Q+1)^{-\gamma} + 2Q^{-\gamma}} \quad (3)$$

For a reuse figure  $N = 7$ , the worst case  $C/I = 17.27$  dB. The minimum value C/I obtained from the simulations is  $\approx 17.024$  dB.

In order to obtain the probability density function of the C/I ratio we start by considering the distance between the home MS and the BTS as a random variable  $r$  and the distance between the  $i$ th interferer and the home BTS as  $d_i$ . The C/I ratio is also a random variable and is given by the ratio distribution of two random variables:

$$\frac{C}{I} = \frac{r^{-\gamma}}{I} \quad (4)$$

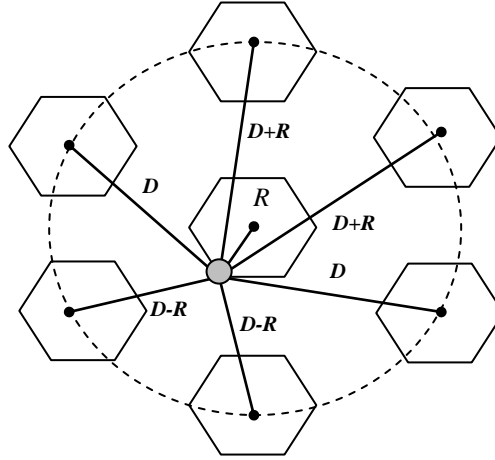


Fig 6 the network configuration for worst case interference scenario

The interference power is given by:

$$I = \sum_{i=1}^6 d_i^{-\gamma} \quad (5)$$

The random variable  $r$  is assumed to be sampled from a uniform distribution. To allow mathematical tractability, the PDF of the variable  $d$  is approximated as a uniform distribution with maximum and minimum distances from the home BTS as  $D+R$  and  $D-R$  respectively. The variable  $\gamma$  is a constant representing the propagation exponent. The PDFs of  $r$  and  $d$  are:

$$pr(r) = \frac{1}{R}, 0 \leq r \leq R$$

$$pd(d) = \frac{1}{2R}, (D-R) \leq d \leq (D+R) \quad (6)$$

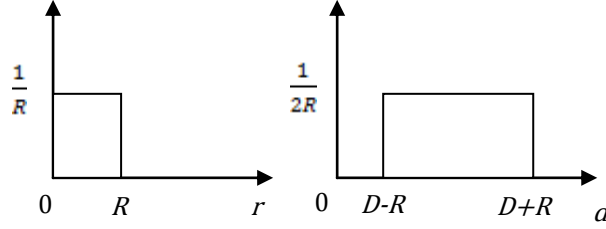


Fig 7 The PDF of the random variables  $r$  and  $d$

The PDF of the random variable  $r^{-\gamma}$  is obtained by applying a transformation process. For a random variable  $x$ , and a one-to-one transformation  $y = h(x)$  is applied to  $x$ , where each value of  $x$  maps to a unique value of  $y$ . To obtain the PDF of  $y$ , we have to get the function  $x = u(y)$  and calculate the Jacobean function:  $J = u'(y)$ . The PDF of  $y$  is:

$$p_y(y) = p_x[u(y)] |J| \quad (7)$$

By applying the transformation, we want to get the PDF of the random variable  $r^{-\gamma}$ :

$$\bar{r} = r^{-\gamma}$$

$$r = \bar{r}^{-\gamma} = u[\bar{r}]$$

$$J = u'[\bar{r}] = \frac{-1}{\gamma} \bar{r}^{-\gamma-1}$$

$$p_r(r) = \frac{1}{\gamma R} \bar{r}^{-\gamma-1}, R^{-\gamma} \leq \bar{r} < \infty \quad (8)$$

Applying the same steps on the random variable  $d$ :

$$p_d(\bar{d}) = \frac{1}{2\gamma R} \bar{d}^{-\gamma-1}, (D+R)^{-\gamma} \leq \bar{d} < (D-R)^{-\gamma} \quad (9)$$

The interference term is given in equation (5), this term is the summation of six independent random variables. The PDF of the summation of two independent random variables is the convolution of their individual PDFs. For six interferers represented by six i.i.d (independent identical distributions), the PDF of the interference is given by:

$$p\left(\sum_{i=1}^6 d_i^{-\gamma}\right) = p_1(\bar{d}) \otimes p_2(\bar{d}) \otimes p_3(\bar{d}) \otimes p_4(\bar{d}) \otimes p_5(\bar{d}) \otimes p_6(\bar{d}) \quad (10)$$

where  $\otimes$  denotes convolution. To simplify the problem and avoid the complicated convolution process, we apply Fourier transform to individual PDFs and multiply them then apply inverse Fourier transform. Let the operators  $F\{\cdot\}$  and  $F^{-1}\{\cdot\}$  denote the Fourier and inverse Fourier transform.

$$p\left(\sum_{i=1}^6 d_i^{-\gamma}\right) = F^{-1}\left\{F\left\{p(\bar{d})\right\}^6\right\} \quad (11)$$

An equivalent solution can be obtained by manipulating the characteristic functions of the random variables. A characteristic function is used to completely describe the PDF. Manipulation of random variables through their characteristic functions simplifies the problem. For a random variable  $x$ , the characteristic function is:

$$\phi_x(t) = E\left\{e^{jxt}\right\} = \int_{-\infty}^{\infty} p(x) \cdot e^{jxt} dx \quad (12)$$

While obtaining the PDF from a characteristic function resembles an inverse Fourier transform process:

$$p_x(x) = \frac{1}{2\pi} \int_{-\infty}^{\infty} \phi_x(t) \cdot e^{-jxt} \cdot dx \quad (13)$$

Thus, the probability density function and the characteristic function are the Fourier transform pairs of each other. An important property of the characteristic function is that the addition of two independent random variables will have a characteristic function equal to the multiplication of the individual characteristic functions. This can be simply concluded by calculating the mean value of the complex exponential with an exponent  $x+y$ :

$$E[e^{j(x+y)t}] = E[e^{jxt} e^{jyt}] = E[e^{jxt}] E[e^{jyt}] \quad (14)$$

Hence, the characteristic function of two added independent random variables is:

$$\phi_{x+y}(t) = \phi_x(t) \cdot \phi_y(t) \quad (15)$$

by extending this relation to a summation of  $n$  i.i.d random variables:

$$Z = \sum_{i=1}^n x_i$$

$$\phi_z(t) = \prod_{i=1}^n \phi_{x_i}(t) \quad (16)$$

Thus, by calculating the characteristic function of a single interferer's random variable  $\bar{d}$

$$\phi_{\bar{d}} = \int_{(D+R)^{-\gamma}}^{(D-R)^{-\gamma}} \frac{1}{2\gamma^R} \cdot \bar{d}^{-\frac{\gamma-1}{\gamma}} \cdot e^{j\bar{d}t} \cdot d\bar{d} \quad (17)$$

Finally, the PDF of the overall interference can be calculated as:

$$p\left(\sum_{i=1}^6 d_i\right) = \frac{1}{2\pi} \int_{-\infty}^{\infty} \phi_{\bar{d}}(t)^6 e^{-j\bar{d}t} \cdot d\bar{d} \quad (18)$$

After calculating the probability density function of both the signal and the six interferers, we have to obtain the probability density function of their ratio. The problem becomes extremely tedious and one would encounter integrals that have no closed form solution. Hence, approximate formulas for the outage probability and C/I ratio statistics are presented in the next section.

#### 2.4. Approximate Analytical Expressions for Carrier-to-Interference ratio PDF in Single and Multiple Interferer Networks

In this section, analytical expressions for the C/I ratio probability density function is developed in order to verify the results obtained from simulations. By considering the basic problem of a single co-cell interferer problem:

$$\frac{C}{I} = \frac{r^{-\gamma}}{d^{-\gamma}} \quad (19)$$

Based on the probability density functions of the random variables  $r$  and  $d$ , the ratio distribution  $r / d$  must be evaluated first in order to get the PDF of the C/I ratio. Assume a new random variable  $u$  that represents the ratio  $u = r / d$ . The joint PDF of the two random variables  $r$  and  $d$  assuming that the two variables are independent is given by  $p(r, d) = p(r) p(d)$  and is plotted in figure 9.

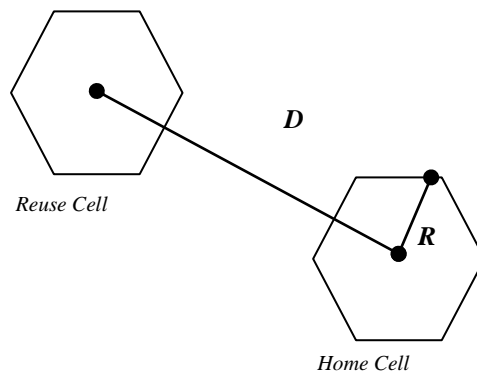


Fig 8 hexagonal cell configuration with single interferer

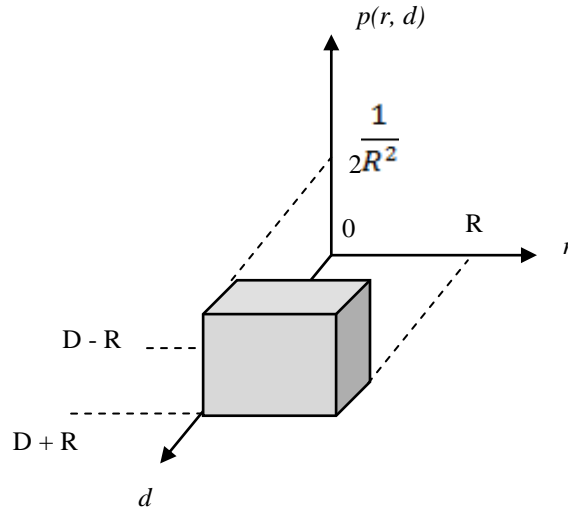


Fig 9 the joint PDF of the distance between the home user and the home cell, and the distance between the interferer user and the home cell

The PDF of the ratio  $u$  can be obtained by differentiating its CDF. For every real number  $u$ , the CDF of the real valued random variable  $r/d$  is given by  $P(r/d \leq u)$ . This is equivalent to evaluating  $P(r \leq ud)$  which means that we need to multiply the area where  $r$  is less than the values bounded by the straight line  $r = ud$  by the uniform PDF amplitude of  $1/2R^2$ . In order to obtain the CDF of  $u$ , we have to split the solution into two regions on the  $u$  axis. The two regions of the  $u$  variable are mapped to two separate integrals on the  $r$ - $d$  plane as shown in figure 11. The first region is when the slope  $u$  of the straight line  $r = ud$  is so large that the straight line crosses the upper border of the  $r$ - $d$  plane (the border identified by the line  $d = D + R$ ), let this region be denoted as region a. The second region is bounded by the straight line that has a small slope causing the line to cross the vertical border  $r = R$ . This region will be denoted as region b. Hence, the CDF and PDF of the random variable  $u$  will have a piecewise definition. Region (a) is obtained when the straight line crosses the horizontal border of the  $r$ - $d$  plane. This is satisfied when  $u(D+R)$  is less than  $R$ . Region (b) is obtained if  $u(D+R)$  exceeds  $R$  and  $u(D-R)$  is less than  $R$ .

**For region (a)**

$$\text{For } 0 \leq u < \frac{R}{D+R}$$

$$P(r \leq ud) = \iint \frac{1}{R^2} dr dd = \frac{1}{2R^2} [2Ru(D-R) + uR \cdot 2R] = \frac{1}{2R^2} [2uD R - 2uR^2 + 2uR^2]$$

$$= \frac{uD}{R}$$

(20)

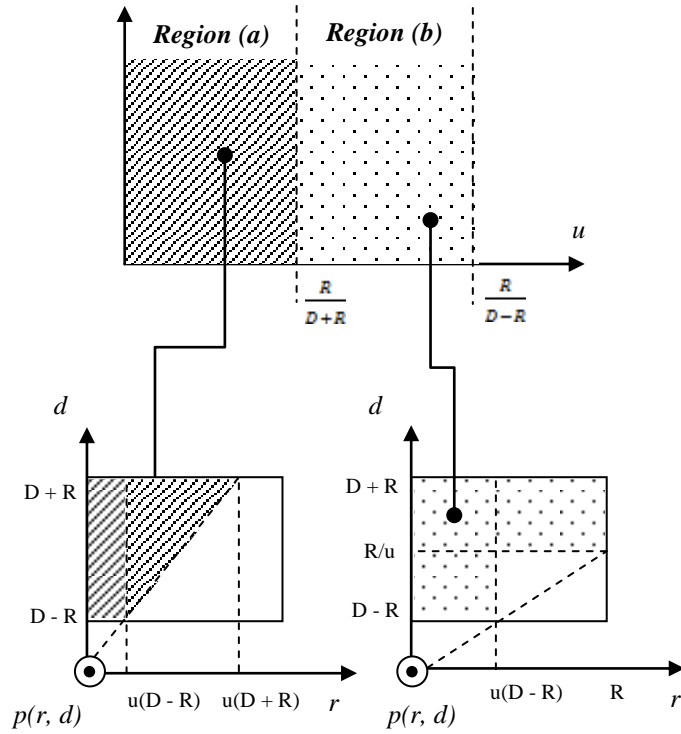


Fig 10 the regions of solution on the r-d plane and its mapping to the u axis

**For region (b)**

$$\text{For } \frac{R}{D+R} \leq u \leq \frac{R}{D-R}$$

$$P(r \leq ud)$$

$$= 1 - \frac{1}{2} \cdot \frac{1}{2R^2} \cdot [R - u(D-R)] \left[ \frac{R}{u} - (D-R) \right]$$

$$= 1 - \frac{1}{2u} [R - u(D-R)] \cdot \frac{1}{2R^2}$$

$$= 1 - \frac{1}{2u} [R^2 - 2uDR + 2uR^2 + u^2D^2 - 2u^2DR + u^2R^2] \cdot \frac{1}{2R^2}$$

$$\begin{aligned}
&= 1 - \frac{1}{4uR^2} [R^2 - 2uDR + 2uR^2 + u^2D^2 - 2u^2DR + u^2R^2] \\
&= \frac{1}{2} + \frac{D}{2R} - \frac{1}{4u} + u \left[ \frac{D}{2R} - \frac{D^2}{4R^2} - \frac{1}{4} \right]
\end{aligned} \tag{21}$$

Thus, the piecewise definition of the cumulative density function is:

$$P(u) = \begin{cases} \frac{1}{2} + \frac{D}{2R} - \frac{1}{4u} + u \left[ \frac{D}{2R} - \frac{D^2}{4R^2} - \frac{1}{4} \right], & \frac{R}{D+R} \leq u \leq \frac{R}{D-R} \\ \frac{uD}{R}, & 0 \leq u < \frac{R}{D+R} \end{cases} \tag{22}$$

The probability density function is the derivative of the cumulative function  $p(u) = \frac{d}{du} P(u)$ , thus, the ratio distribution is given by:

$$p(u) = \begin{cases} \frac{1}{4u^2} + \left[ \frac{D}{2R} - \frac{D^2}{4R^2} - \frac{1}{4} \right], & \frac{R}{D+R} \leq u \leq \frac{R}{D-R} \\ \frac{D}{R}, & 0 \leq u < \frac{R}{D+R} \end{cases} \tag{23}$$

Recall that the quality reuse ratio  $Q$  is given by  $Q = \frac{D}{R}$ , thus, the probability density function can be reformulated as:

$$p(u) = \begin{cases} \frac{1}{4u^2} - \left( \frac{Q-1}{2} \right)^2, & \frac{1}{Q+1} \leq u \leq \frac{1}{Q-1} \\ Q, & 0 \leq u < \frac{1}{Q+1} \end{cases} \tag{24}$$

Note that the expression presented in (24) satisfies all the properties of a PDF: the PDF integrates to unity over the  $u$  domain  $\int_{-\infty}^{\infty} p(u) du = 1$  and continuity of the function is maintained at  $\frac{1}{Q+1}$ , note that the PDF vanishes at  $\frac{1}{Q-1}$ .

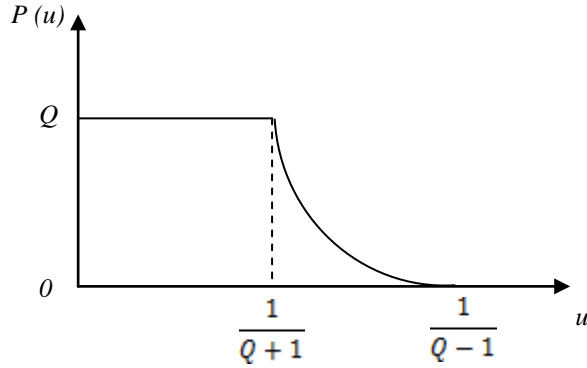


Fig 11 the ratio distribution as a function of the quality reuse ratio

By evaluating the mean and the variance of this PDF, we obtain:

$$\mu = \frac{1}{4} \ln \left| \frac{Q+1}{Q-1} \right| \quad (25)$$

$$\sigma^2 = \frac{1/3}{Q^2 - 1} - \frac{1}{16} \left( \ln \left| \frac{Q+1}{Q-1} \right| \right)^2 \quad (26)$$

By applying a non-linear transformation for the random variable raised to the path loss exponent;  $Z = \left(\frac{r}{d}\right)^{-\gamma}$  and thus,  $\frac{r}{d} = Z^{-1/\gamma}$ . The Jacobean  $|J| = \frac{-1}{\gamma} Z^{-\left(\frac{1}{\gamma}+1\right)}$ , the PDF of the transformed variable Z is given by  $p(Z) = p[u(Z)] |J|$ , thus, the PDF of Z is:

$$p(Z) = \begin{cases} \frac{Z^{\left(\frac{1}{\gamma}-1\right)}}{4\gamma} - \frac{1}{\gamma} \cdot \left(\frac{Q-1}{2}\right)^2 \cdot Z^{\left(\frac{1}{\gamma}-1\right)}, & (Q-1)^\gamma \leq Z \leq (Q+1)^\gamma \\ \frac{Q}{\gamma} \cdot Z^{-\left(\frac{1}{\gamma}+1\right)}, & (Q+1)^\gamma \leq Z < \infty \end{cases} \quad (27)$$

The result obtained in equation (27) represents the probability density function of the Carrier-to-Interference ratio for a single interferer network. The lower bound on the ratio Z is equal to  $(Q-1)^\gamma$  represents the worst case interference when the home user is at the home cell border (at a distance R from the home base station) and the interferer is at the nearest point to the home BTS (at a distance  $D-R$  from the BTS). In this case the ratio  $C/I = (R^{-\gamma} / (D-R)^{-\gamma}) = ((D-R)^\gamma / R)^\gamma = (D/R - 1)^\gamma = (Q-1)^\gamma$ . On the other hand, the maximum possible ratio is attained when the home cell is coinciding with the home base station leading to an infinite C/I ratio. Let the variable  $Z = CIR$  denote the Carrier-to-Interference ratio, the outage probability is defined as:

$$P(CIR \leq \varepsilon) = \int_{-\infty}^{\varepsilon} P_{CIR}(CIR) dCIR \quad (28)$$

For  $\varepsilon \leq (Q + 1)^\gamma$ , the outage probability is:

$$\begin{aligned} P_{\text{out}} &= \int_{-\infty}^{\varepsilon} \frac{1}{4\gamma \cdot \text{CIR}} [ \text{CIR}^{\frac{1}{\gamma}} - (Q - 1)^2 \cdot \text{CIR}^{-\frac{1}{\gamma}} ] d\text{CIR} \\ &= \frac{1}{4} [ \varepsilon^{\frac{1}{\gamma}} + (Q - 1)^2 \varepsilon^{-\frac{1}{\gamma}} - 2(Q-1) ] \end{aligned} \quad (29)$$

Notice that the outage probability for a certain threshold  $\varepsilon$  increases as the quality reuse ratio  $Q$  increases. The outage probability for  $\varepsilon > (Q + 1)^\gamma$

$$\begin{aligned} P_{\text{out}} &= \int_{(Q-1)^\gamma}^{(Q+1)^\gamma} P(\text{CIR}) d\text{CIR} + \int_{(Q+1)^\gamma}^{\varepsilon} \frac{Q}{\gamma} \text{CIR}^{-\left(\frac{\gamma+1}{\gamma}\right)} d\text{CIR} \\ &= \frac{Q}{\gamma \cdot -\left(\frac{1}{\gamma}\right)} \text{CIR}^{-\left(\frac{1}{\gamma}\right)} \Big|_{(Q-1)^\gamma}^{\varepsilon} + \frac{1}{4} (Q+1) + \frac{1}{4} (Q-1) 2 (Q+1) - 1 \\ &= Q \left[ \frac{1}{Q+1} \cdot \varepsilon^{-1/\gamma} \right] + \frac{1}{4} [(Q+1) + \frac{(Q-1)^2}{Q+1} - 2(Q-1)] \end{aligned} \quad (30)$$

Thus, the piecewise definition of the outage probability is given by:

$$P_{\text{out}} = \begin{cases} \frac{1}{4} \left[ \varepsilon^{\frac{1}{\gamma}} + (Q - 1)^2 \varepsilon^{-\frac{1}{\gamma}} - 2(Q - 1) \right] \\ \quad , \varepsilon \leq (Q + 1)^\gamma \\ Q \left[ \frac{1}{Q+1} - \varepsilon^{-\frac{1}{\gamma}} \right] + \frac{1}{4} \left[ (Q + 1) + \frac{(Q-1)^2}{Q+1} - 2(Q - 1) \right] \\ \quad , \varepsilon > (Q + 1)^\gamma \end{cases} \quad (31)$$

The expression obtained in (31) is valid only for the single interferer scenario. For the case of six independent interferers, we can apply the Union Bound principle (Boole's Inequality), which states that for a set of events  $A_i$ :

$$P(\bigcup_i A_i) \leq \sum_i P(A_i) \quad (32)$$

Thus, for six independent and identical interferers, the outage probability is approximated as:

$$P_{\text{out}} \leq \begin{cases} \frac{3}{2} \left[ \varepsilon^{\frac{1}{\gamma}} + (Q - 1)^2 \varepsilon^{-\frac{1}{\gamma}} - 2(Q - 1) \right] \\ \quad , \varepsilon \leq (Q + 1)^\gamma \\ 6Q \left[ \frac{1}{Q+1} - \varepsilon^{-\frac{1}{\gamma}} \right] + \frac{3}{2} \left[ (Q + 1) + \frac{(Q-1)^2}{Q+1} - 2(Q - 1) \right] \\ \quad , \varepsilon > (Q + 1)^\gamma \end{cases} \quad (33)$$

### 1. Approximation of the DTX and PC C/I gain

As discussed before, the DTX and PC features in GSM help to reduce the interference power, allowing the network operator to reduce the reuse factor without losing quality and thus increasing the network's capacity. In this section, we aim at verifying the values of the C/I gains obtained from DTX and PC from the Monte Carlo simulation by deriving approximate formulas for them.

DTX is used to lower the transmitted power during the user's silence frames. The percentage of non-silent speech frames (with duration T) is known as the VAF (Voice Activity Factor)  $\eta$ . Assume a discrete binary Random Process  $\sigma(t=nT)$  that describes whether the current TDMA frame carries speech or not. This process will follow the Probability Mass Function (PMF):

$$F(\sigma) = \begin{cases} \eta & , \sigma = 1 \\ 1 - \eta & , \sigma = M \end{cases} \quad (34)$$

where  $M$  is the DTX attenuation factor ( $M < 1$ ) and  $\sigma$  is a random variable describing the attenuation in a certain speech/silence frame. The home MS and the six interferers form the *ensemble* of this random process. The random process is a function of time and emits either 1 or  $M$  for every frame transmitted by user equipment. The temporal mean of this random process is intuitively given by:

$$\langle \sigma(t) \rangle = \eta + (1 - \eta)M \quad (35)$$

Equation (35) describes the time mean of the random process shown in figure 12. The attenuation is 1 in a fraction  $\eta$  of the frames and the attenuation is  $M$  in  $(1-\eta)$  of the frames. Thus, the average attenuation value is  $(1-\eta)M + \eta$ . Because we calculate the C/I ratio per frame, and assuming that the random process is ergodic, the ensemble mean at time  $t$  is equal to the temporal mean. In every time instant,  $\eta$  interferers transmit with full power and  $(1-\eta)$  others have an attenuation of  $M$ . Thus, the interference power is averaged to be  $(1-\eta)M + \eta$  per frame, the DTX gain is then equal to the time and ensemble averages:

$$\begin{aligned} \text{DTX gain} &= \langle \sigma(t) \rangle_{\text{dB}} = \overline{\sigma(t)}_{\text{dB}} \\ &= -10 \log_{10} (\eta + (1 - \eta)M) \end{aligned} \quad (36)$$

For an attenuation of  $M = 10$  dB and a voice activity factor of 40 %, the DTX gain is 3.372 dB which matches the results obtained from the Monte Carlo simulation.

By enabling the Power Control (PC) feature, the transmitted signal from a MS depends on the location of the user relative to its associated BTS. The hexagonal cell is divided into seven concentric rings with the farthest ring transmitting with full power, and each transition between two rings cause a 2 dB attenuation of the transmitted power. The PMF of the PC attenuation is shown in figure 13. The C/I ratio can be given as:

$$\frac{C}{I} = \frac{P r^{-\gamma}}{\sum_{i=1}^6 P_i d_i^{-\gamma}} \quad (37)$$

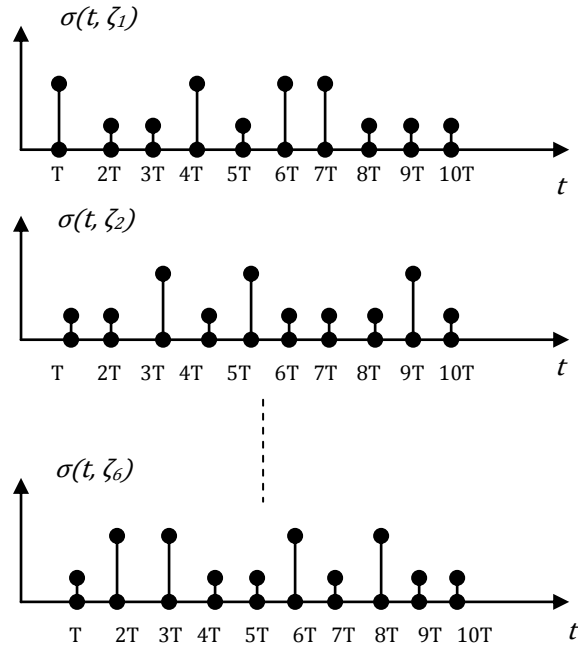


Fig 12 the DTX attenuation ensemble for the six interferers

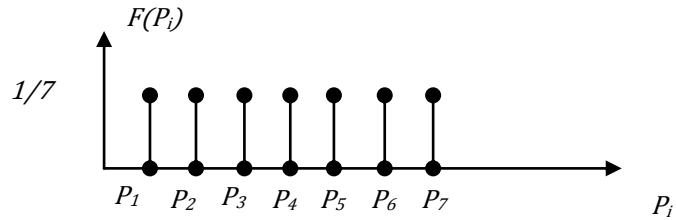


Fig 13 the PMF of the Power Control attenuation

The analytical expression for the outage probability with PC is very difficult to obtain as we have a new random variable  $p$  plugged into the equation, and extra variable transformations must be applied. However, an approximate bound for the PC gain can be obtained. The PC results in interference averaging; the average PC attenuation is:

$$P_{avg} = \sum_{i=1}^7 \frac{P_i}{7} \tag{38}$$

The best scenario for the C/I is when no attenuation due to PC (the MS is at farthest point to the BTS):

$$PC \text{ gain} \leq 10 \log_{10} \left( \sum_{i=1}^7 \frac{P_i}{7} \right) \tag{39}$$

For the case of 2 dB attenuation step between each two concentric rings, the approximate gain bound is 4.14 dB, while the gain attained is 3 dB.

### 3. Frequency Hopping

Increasing the capacity of the cellular system is achieved by reducing the reuse figure. However, a lower reuse figure will cause a high level of cochannel interference.

The reduction of reuse factor must be associated with interference mitigation techniques to compensate the expected loss of quality due to the increased cochannel interference. In section II, we presented PC and DTX techniques to improve the outage C/I ratio. Another technique for interference mitigation in GSM is Frequency Hopping. Frequency Hopping (FH) is a process of changing the RF carrier frequency in a prescribed rate. GSM adopts slow FH transmission, where the RF carrier is changed for every new burst. Besides, the RF carrier selection is done on a random basis rather than cyclic one. In contrast to Cyclic FH, random FH offers worse frequency utilization and better interference diversity. Assume that we have a hopping sequence with 8 RF carriers, in a set of 8 frames, random hopping would result in the selection of 5 frequencies only, unlike cyclic hopping where all the 8 frequencies would be used [2]. Thus, frequency diversity in cyclic FH is better than random hopping. However, in cyclic FH, the user and the cochannel interferers may keep transmitting at the same RF carrier for several consecutive bursts. This is not possible in random FH, where interference averaging results from interference diversity. While cyclic FH network has to be designed based on the worst case interference, random FH is designed based on the average interference.

#### 3.1. Generation of the Frequency Hopping Sequence

In this section, the FH sequence generation algorithm is presented. The algorithm complies with the GSM specifications [3]. The following parameters are used to determine the hopping sequence:

- **MAI (Mobile Allocation Index):** The MAI is obtained through a sequence generation algorithm. It is used to index an MA table that maps it to an RF channel.
- **MA (Mobile Allocation):** The MA is the look up table giving the relation between different MAI (index) numbers and the corresponding RF channel numbers (ARFCN).
- **MAIO (MAI offset):** An offset in the MAI used to generate a shifted hopping sequence; this is specific for each transceiver and offers uncorrelated hopping sequence for each MS within the same site to avoid intra-cell interference.
- **HSN (Hopping Sequence Number):** A number that specifies the hopping sequence used. This number varies from cell to cell but is constant for each cell. Cyclic hopping occurs when HSN = 0.
- **T1, T2 and T3:** are internal timers to create the hopping sequence periodicity. The hopping sequence has a period of 84863.
- **Frame Number (FN):** A number that is incremented per TDMA frame and triggers the T1, T2 and T3 timers, where:

$$T1 = FN \text{ mod } 64$$

$$T2 = FN \text{ mod } 26$$

$$T3 = FN \text{ mod } 51$$

The flow chart in figure 14 depicts the sequence generation algorithm. The frequency utilization in cyclic hopping and random hopping are compared in figure 15. In cyclic hopping, a sequence of N possible RF carriers are utilized every N bursts. While in random FH, utilization decreases and thus, frequency diversity is better in cyclic hopping (HSN = 0).

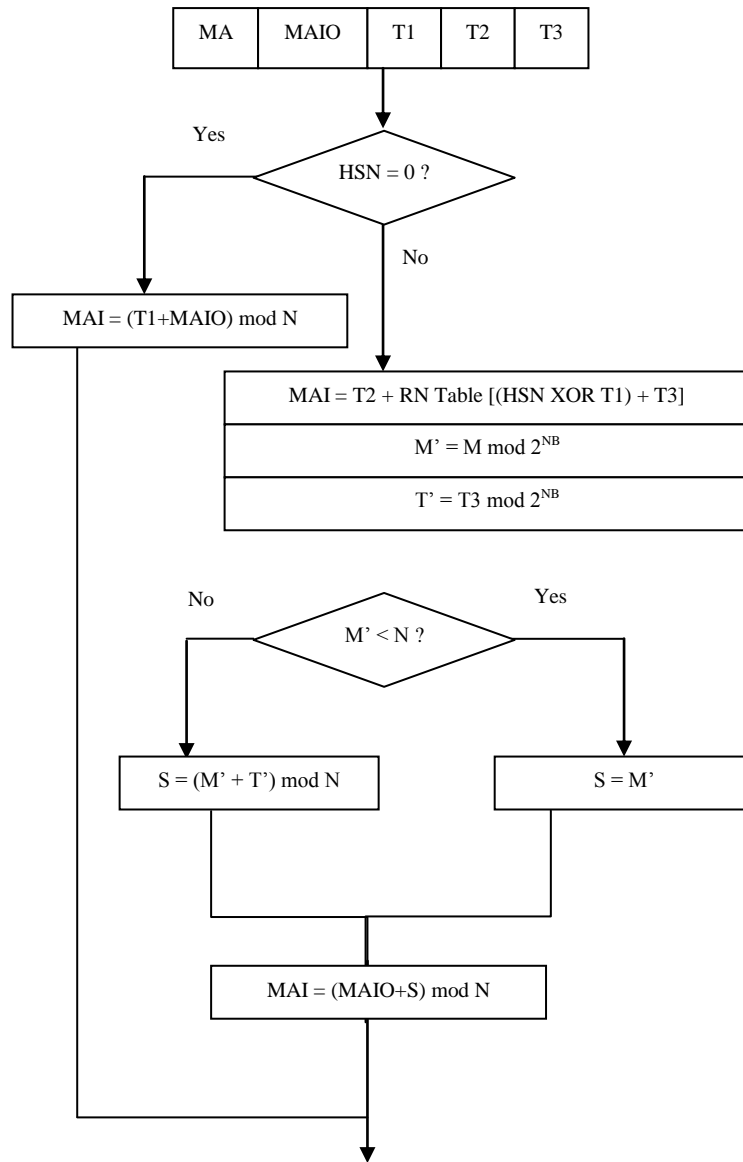


Fig 14 the flow chart for hopping sequence generation. Courtesy of [3]

### 3.2. Effect of random FH on the Carrier-to-Interference ratio

As discussed before, random FH introduces the interference diversity effect, which results in interference averaging. The C/I ratio is boosted due to the averaging of the interferer power over time. The C/I ratio statistics (PDF and CDF) are obtained via Monte Carlo simulation for random FH. Because the multipath effects and frequency selective fading were not included yet, the frequency diversity has no impact on the results obtained from this simulation.

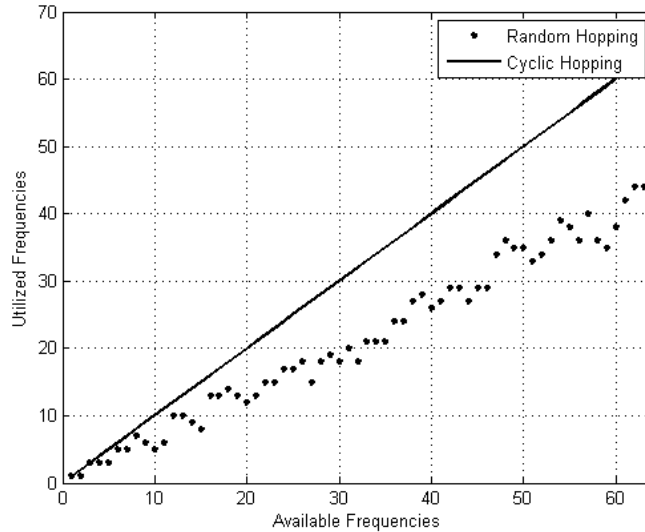


Fig 15 comparison of the frequency utilization in cyclic and random frequency hopping schemes

The Monte Carlo simulations are carried out with the following settings: every co-cell has a different HSN number to generate a different hopping sequence, the  $N$  users within each co-cell are active with probability of  $LSB$  users, where  $N$  is the number of hopping frequencies and  $LSB$  is the system load (the percentage of utilized channels). Within each cell, all users have the same hopping sequence but with a frequency offset, realized by varying their MAIO number. The MS instances generated for Monte Carlo simulation are kept alive for a specific period of time (statistically sufficient to demonstrate the interference averaging effect) to measure the average  $C/I$  ratio. Note that the collision between the home MS and the interferers is function of the number of hopping frequencies and the system load. As the number of available hopping frequencies increase, the probability of collision decreases. The effect of system load is decreasing the probability of collision as the load decreases. Hence, the maximum interference diversity gain is expected in networks with fractional load and tight frequency reuse [4][5]. Simulations for 8 hopping frequencies and various system loads are plotted in figure 16. As shown in the figure, decreasing the system load shifts the mean  $C/I$  curve to the right, which means that we obtain  $C/I$  performance gain for systems with low load. A 100% load means that there will be no interference diversity and we retain the  $C/I$  CDF of the case when no hopping occurs.

### 3.3. Impact of FH on the Quality of Service (QoS)

In systems with fixed or cyclic hopping, the Bit Error Rate and Frame Erasure Rate (BER, FER) can be mapped uniquely to the mean Carrier-to-Interference ratio observed on the radio link [2][4]. This one-to-one mapping is also independent of the system load. For these reasons, we approved the  $C/I$  value satisfying a 10% outage probability as a direct measure of the perceived QoS. On the other hand, in random FH systems, the  $C/I$  ratio is a stochastic process where interference diversity doesn't only reduce the mean  $C/I$  ratio, but also changes the distribution of the interference; different bursts perceive different  $C/I$  ratios. This distribution would definitely have an impact on the FEC (Forward Error Correction) performance and other Physical layer functions of GSM transceivers. Based on this, the mapping between mean  $C/I$  and the BER/FER is not unique and the same mean  $C/I$  may result in different Error rates due to the varying interference distribution. Thus, QoS can't be directly related to the mean  $C/I$ , but we have to estimate the FER resulting from mean  $C/I$  and interference distribution, and then the QoS can be related to the obtained FER statistics.

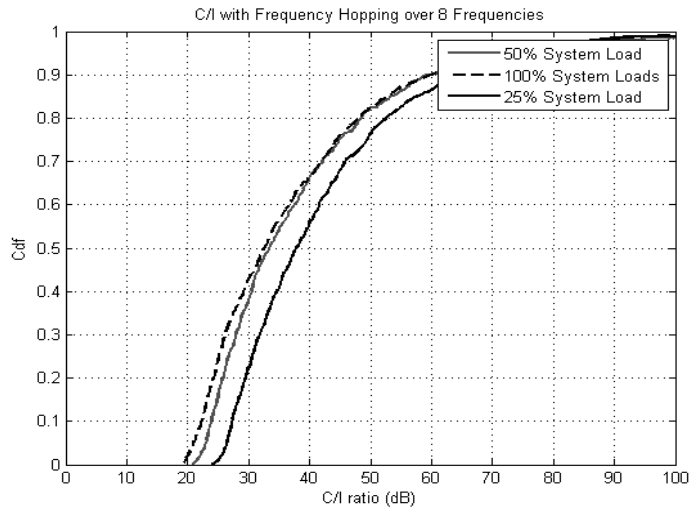


Fig 16 C/I performance gains are obtained for system loads of 25%, 50% and 100%.

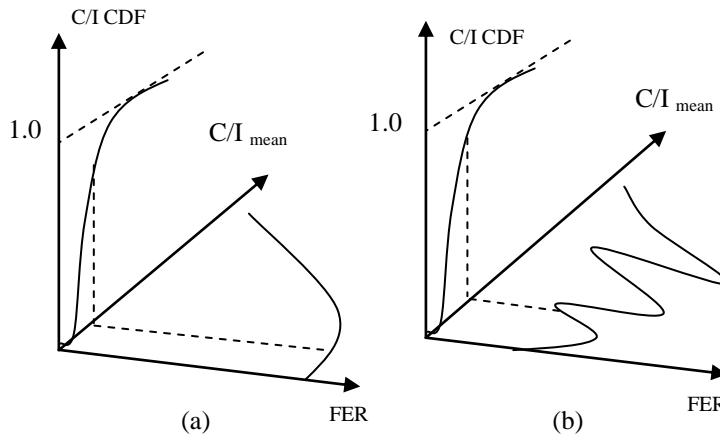


Fig 17 (a) the mapping of mean C/I to FER is unique in non-hopping or cyclic hopping system (b) mapping of C/I and FER depends on the interference distribution

In order to evaluate the FER and BER, a link level model has to be developed. This link level model includes the bit interleavers, Viterbi equalizer, channel coding and modulation. The usage of an actual physical layer model, will introduce extreme complexity to the Monte Carlo simulation. Instead of an actual link level model, a statistical interface between system and link level models is used. A simple approach is presented in [6], [7] and [8], the output of the system level part of the simulator, expressed in signal to interference values, is used as input for look up tables, which lead to a BER and a Frame Erasure Rate (FER) for each radio link. The link model is simply a Statistical Link Level Mapper (SLLM) that maps C/I mean values and distributions to corresponding FER. The two-step mapping procedure is applied by first mapping the C/Iburst (Signal to Interference ratio over a burst) obtained from the system level model to a corresponding number of erroneous bits in the burst. Then, the Bit Errors are grouped to compose a frame and we decide whether the frame is erased or not based on common link level statistics. Figure 18 is a block diagram that depicts the integrated System and Link level models. The link level model's results incorporated with the system model are dependent on the channel and simulation conditions. Hence, a disadvantage of this model is that we can never

obtain link level FER and BER performance curves for all possible channel conditions, and the obtained results will normally be limited to a certain degree of accuracy. As discussed before, the link level BER and FER curves are dependent on the channel model. The next section presents the adopted simulation settings; channel model, shadowing model and path loss model. The interference diversity gain will be calculated based on the statistical model presented in this section together with the simulation environment discussed in the next section.

#### 4. Simulation Environment

Practical considerations for simulating the system and link level GSM models include: Antenna Radiation Patterns, the Path loss model, the Shadowing (large scale fading) model, and the Multipath propagation profile. The selection of these models and parameters would affect the reference statistical link level curves that are used for interfacing with the system model. In our simulations, we consider a reuse factor of  $N = 7$ , a path loss exponent  $\gamma = 4$ , a cell radius of 1 km and a completely interference limited system. Adjacent Channel Interference (ACI) is neglected. We assume 3-sector based sites.

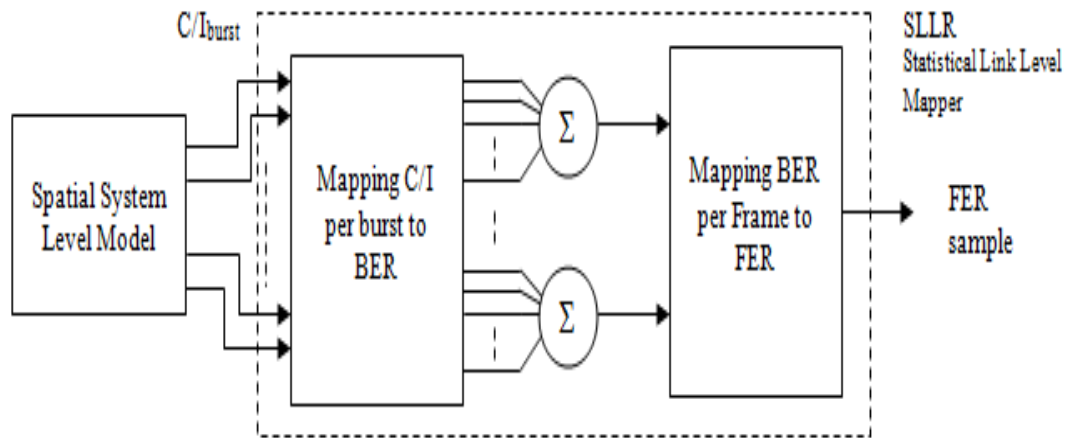


Fig 18 a block diagram for the integrated system and link level models

##### 4.1. Antenna Radiation Pattern

A practical antenna radiation pattern is incorporated in the system level model. The antenna has 10 dB beam-width of 120°. The antenna is suitable for 3-sector sites. Employing 3-sector sites into the network would decrease the number of interferers from 6 to 2. Thus we expect a boost in the C/I outage ratio by  $10 \log_{10}(4) = 6$  dB. This gain is not exactly achieved as the rejected interferers are not completely suppressed at the BTS due to the non-zero gain of the sector antenna. After re-plotting the C/I DF curve, a 10% outage is satisfied at 19.26 dB (corresponds to a gain of 5.26 dB compared to the Omni-directional cells case).

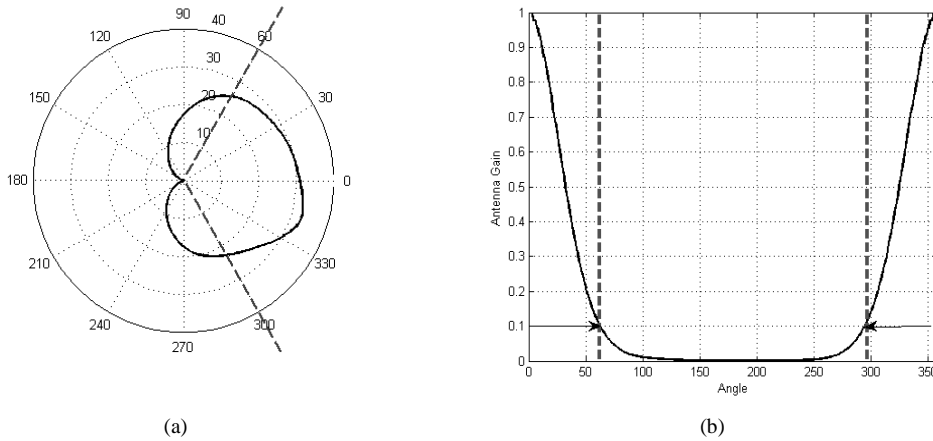


Fig 19 (a) a polar plot of the sector antenna horizontal plane radiation pattern (b) linear plot of the antenna gain versus the spatial angle. Courtesy of Vodafone Egypt

#### 4.2. Pathloss Model

The pathloss model describes attenuation observed in the mean received power as function of distance and path loss exponent. As defined in the GSM Radio transmission and reception specifications [9] the path loss is defined as:

$$L[\text{dB}] = 18.8 + \gamma \log(d[\text{m}]) \quad (40)$$

#### 4.3. Large Scale Fading (Lognormal Shadowing)

The large scale fading (shadowing) due to obstacles intercepting the signal in its way to the receiver is usually modeled as a log-normal random variable. The log-normal probability density function characterizes a random variable  $x$  if  $\log(x)$  follows a normal distribution. The overall attenuation has a mean value equivalent to the path loss and fluctuations decided by the standard deviation of the log-normal shadowing. According to GSM 03.30 [9] the standard deviation  $\sigma_F$  is set to 7.

#### 4.4. Multipath Propagation Profile

The multipath propagation results in fast fading (also known as small scale fading). The spatial interference between different reflected versions of the signal may be constructive or destructive. This leads to spatial variations in the received power, and with a moving receiver, the power fluctuations become also time variant. The Power Delay Channel Profiles (PDP) adopted in simulations are typical TU3 and TU50 [10] (Typical Urban Models with speed of 3 km/hr and 50 km/hr) in addition to rural environments model (RA model). A Rayleigh distribution is assumed for the temporal channel gain. It is assumed that the hop size is greater than the channel coherence bandwidth and the burst duration is greater than the coherence time of the channel. Based on this, we consider a new channel gain for each burst (hop) sampled from a 2-Dimensional time-frequency channel response and a constant lognormal shadow fading gain for every frame. Note that the frequency hopping alters the observed frequency selective fading pattern. This frequency diversity effect is useful for the FEC (Forward Error Correction) as it diversifies the corrupted bursts. The TU channel model is applicable for dense urban areas, where numerous multipath components cause frequency selective channel

behavior. This model is not applicable for all practical environments. In Rural, low population areas, the RA (Rural Areas) Model better describes the channel response. Only six channel taps are included with quite less delay spread and a frequency flat response.

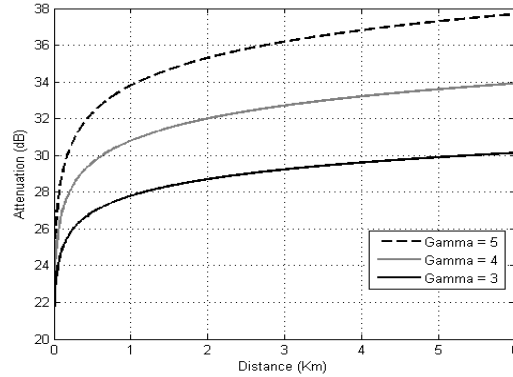


Fig 20 the path loss attenuation in dB plotted versus distance for various value of the path loss exponent

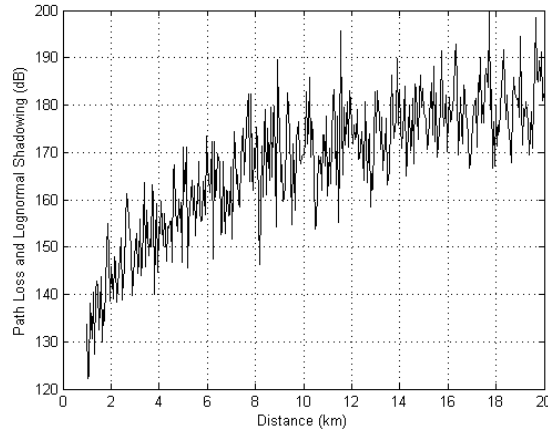


Fig 21 the overall path loss and lognormal shadowing with a standard deviation of 7 dB.

The 2D time-frequency channel grid is obtained as follows: a train of impulses with a period of  $N$  samples is applied to the channel. The resultant signal observed at the channel output is a train of impulse responses. Because the channel is time variant, this train doesn't have an identical output every  $N$  samples. The number of samples  $N$  is chosen to be the same as the number of hopping frequencies and the period of the impulse train must be smaller than the coherence time. The output train of impulse responses is segmented into frames of  $N$  samples and every frame is applied to an  $N$ -point FFT (Fast Fourier Transform) operation to obtain the channel transfer function. The obtained FFT frames are arranged sequentially in a 2D matrix giving a two dimensional channel representation. Each row represents a temporal index identifying a specific burst, while each column is a frequency bin. The values composing a row show how the gain associated with this frequency component varies with time. Because the MS is kept alive for a specific period of time for each Monte Carlo simulation instance, the fast fading gain observed by a certain MS at a certain time instant is decided by the burst index and the current hopping frequency. Those two indexes extract a channel gain from the 2D channel matrix.

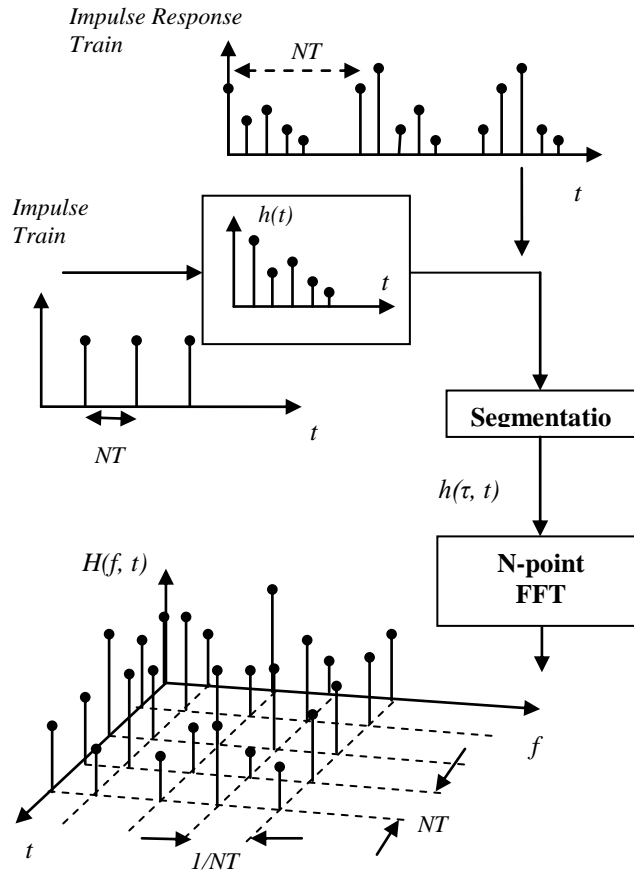


Fig 23 the 2D channel matrix generation block diagram

Various time-frequency fading channel grids are presented in figures 24, 25 and 26. Figure 14 shows a time-invariant TU channel. When the receiver is stationary, the channel impulse response is kept constant and no variations in the channel gain are encountered for different bursts. Because the delay spread of the TU model is relatively large, the channel is frequency selective. When the receiver is moving with a considerable speed, the transfer function becomes time variant (TU3 and TU50 models). Figure 25 shows a frequency selective channel encountered by a moving receiver. Every burst encounters a new channel response. Frequency hopping would have a desirable effect in frequency selective channels. Due to the presence of frequencies with deep fades, consecutive bursts are corrupted in a fixed hopping scheme. However, in frequency hopping networks, different bursts are transmitted at different frequencies and thus, if a burst is subjected to a fading dip, the next burst is unlikely to be faded. This effect is called frequency diversity and is far more significant for slow moving receivers. For fast moving receivers, the channel gain varies drastically for every burst, and frequency diversity becomes inherited from the channels extremely short coherence time. The Rural channel models (RA models) have less delay spread values and thus a flat frequency response is offered by RA channels. Figure 26 shows a typical RA flat channel where the gain for all frequency components is the same and varies with time for moving receivers. In RA channels, frequency diversity has no impact on the system performance as all frequencies have the same channel gain.

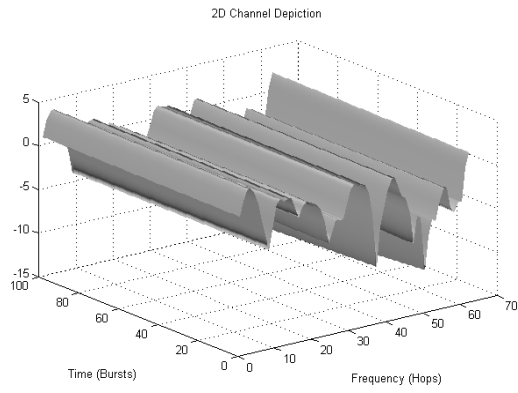


Fig 24 a time-invariant frequency selective channel (stationary receiver)

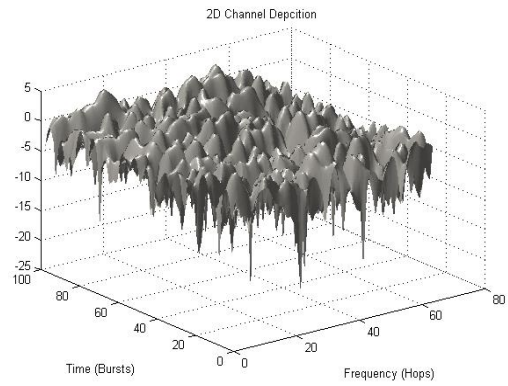


Fig 25 a frequency selective time variant TU channel model

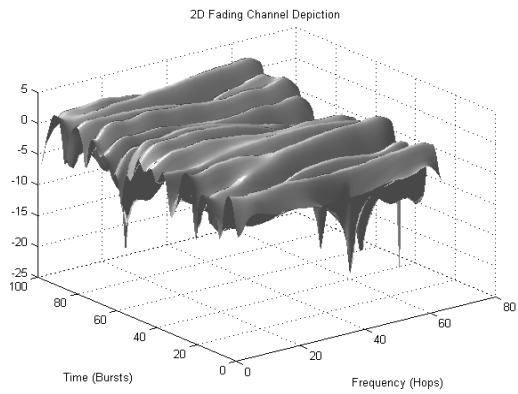


Fig 26 a frequency-flat time-variant RA channel model

## 5. Impact On Frequency Planning and Spectral Capacity Calculation

The implications for frequency planning are obvious; to make the best usage of frequency hopping, the system should be planned with as tight frequency reuse as possible. The system can be designed with a low system load without loss of capacity. Furthermore, it allows hopping over many frequencies. In this section the Hard and Soft blocking limits are defined, the effect of the system load and number of hopping frequencies on the system's FER is shown, the improvements in the C/I statistics due to interference diversity is discussed and finally we introduce the Spectral Capacity as a qualitative assessment parameter for the operator's revenue compared to investment cost. The objective of this section is to verify that interference mitigation techniques (PC, DTX and FH) can allow reducing the reuse figure of the network preserving the call quality expressed in terms of the FER.

### 5.1. Hard and Soft Blocking Limits

The capacity of a network with a specific reuse figure is limited by a certain QoS criterion. There are two basic QoS criteria [2]:

- **Hard blocking limit:** This is also known as *blocking due to no resources available* (in the call setup phase). The capacity is limited by the amount of traffic that causes 2 % blocking probability experienced by users. This is calculated by the *Erlang-B Formula*.
- **Soft blocking limit:** Represents the *call failure due to low link quality* (or equivalently high interference power in the connected mode). It is characterized by performance parameters' thresholds such as C/I, BER and FER. Usually the C/I is required to be greater than 9 dB or the FER is less than 2 % in 90% in the service area.

Hence, for each reuse scheme, we have to check whether it is interference limited or limited by blocking probability. Based on this, we calculate the maximum affordable system load (either from Erlang-B formula or from FER curves).

### 5.2. Impact of System load and Number of Hopping Frequencies on FER performance

The impact of the system load on the CDF of the FER in a Frequency Hopping scenario was studied. It was found that interference diversity is improved when the system load decreases [11]. For a constant number of hopping frequencies, the less load on the system, the less likelihood that the interferers are using the same frequency of the home cell for transmission. As shown in figure 27, a FH system with 8 hopping frequencies with 3/9 reuse pattern is studied. The CDF of the FER is plotted for system load of 25%, 50% and 100%. It is obvious that the FER < 2% criterion is satisfied for a larger service area when the system load is low. The impact of the number of hopping frequencies is also studied for the same reuse pattern with 2, 4 and 8 hopping frequencies. As shown in figure 28, increasing the number of hopping frequencies results in an improvement of the FER CDF. A larger portion of the service area experiences a FER less than 2% when the number of hopping frequencies is increased. Thus, it is desirable that FH networks have low system loads with large number of hopping frequencies. This corresponds to adopt fractional loading and a tight reuse pattern.

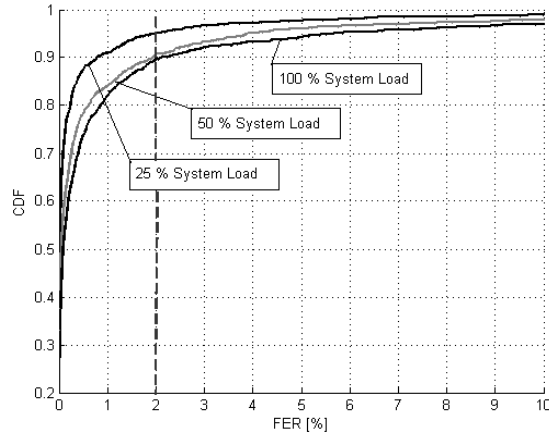


Fig 27 impact of the system load on the FER performance in a TU3 channel

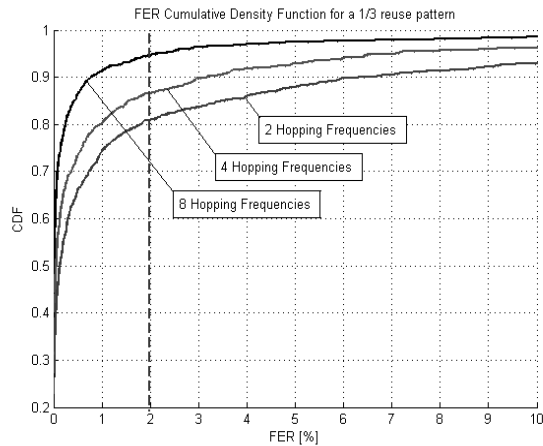


Fig 28 impact of the number of hopping frequencies on the FER performance in TU3 channel

### 5.3. Carrier-to-Interference ratio aggregated gain due to DTX, PC and FH

As stated before, interference mitigation techniques improve the  $C/I$  statistics and relax the soft blocking limit. By applying slow fading, fast fading and path loss for a 3/9 reuse pattern scheme with 3 sector sites, the  $C/I$  gain at 10% outage was evaluated due to DTX, PC and FH. Without any features, the  $C/I$  ratio satisfied at 10% outage is 11 dB. By enabling Discontinuous transmission, Power control and Frequency Hopping with 8 hopping frequencies and 25% system load, the  $C/I$  ratio at 10% outage is boosted to 20 dB. This corresponds to 9 dB aggregated gain due to the three interference mitigation techniques.

### 5.4. Spectral Capacity Calculation

The Spectral Capacity  $\eta$  of a cellular network is obtained by relating the capacity (revenue) to the network investment costs spent for the licensed spectrum and building up of the network structure. The spectral capacity is calculated as [2]:

$$\eta = \frac{1}{B} \cdot \lambda_{\text{cell}} \cdot N_{\text{sec}} \quad (40)$$

B : system bandwidth allocated to the operator (Hz)

$\lambda_{\text{cell}}$  : Traffic in Erlang

$N_{\text{sec}}$  : Number of sectors per site

Our goal is to compare the spectral capacity of the conventional 4/12 reuse GSM network with a 3/9 reuse pattern network that adopts DTX, PC and FH. The spectral capacity is calculated based on the maximum offered traffic imposed by either hard or soft blocking limits. It is expected that, without loss of signal quality, a capacity gain is achieved due to the reduced reuse factor. The capacity gain is quantified in terms of spectral capacity as it relates network operator's revenues to the investment costs. Assume that the GSM Network operator has an allocated bandwidth of 14.4 MHz. As the bandwidth of the single GSM channel is 200 kHz, we have a total of 72 RF channels per cluster. In a 4/12 reuse pattern, this corresponds to 6 RF channels per sector. The TDMA frame can hold 8 users resulting in a total number of 48 channels. Because a fully loaded 4/12 reuse scheme can pass the FER criterion, the system is thus subjected to the hard blocking limit. By substituting the Erlang-B formula with 48 channels per sector and 2% blocking, the offered traffic is found to be 38.35 Erlang/sector (115 Erlang/site). By substituting in equation (40), the spectral capacity is found to be 8 Erl/(site-MHz). By adopting a 3/9 reuse scheme, then we have a total of 8 RF channels per sector, and thus, 8 hopping frequencies are employed. The maximum system load that keeps the FER < 2 % for 90 % of the service area is 75%. This corresponds to  $0.75 \times 8 \times 8 = 48$  Erlang/sector (144 Erlang/site). The spectral capacity becomes 10 Erl/(site-MHz). Thus, a capacity boost with a factor of 1.25 is achieved without loss of quality when PC, DTX and FH are applied to the 3/9 reuse scheme.

Table 3 spectral capacity calculation for 4/12 and 3/9 reuse schemes

<b><i>Blocking Scenario</i></b>	<b><i>4/12 reuse with hard blocking limit</i></b>	<b><i>3/9 reuse with soft blocking limit</i></b>
Number of RF channels per sector	6	8
Actual number of channels per sector	48	64
Traffic per sector	38.35 Erlang	$0.75 \times 64 = 48$ Erlang
Traffic per site	115 Erlang	144 Erlang
Spectral Capacity	8 Erl/(site-MHz)	10 Erl/(site-MHz)

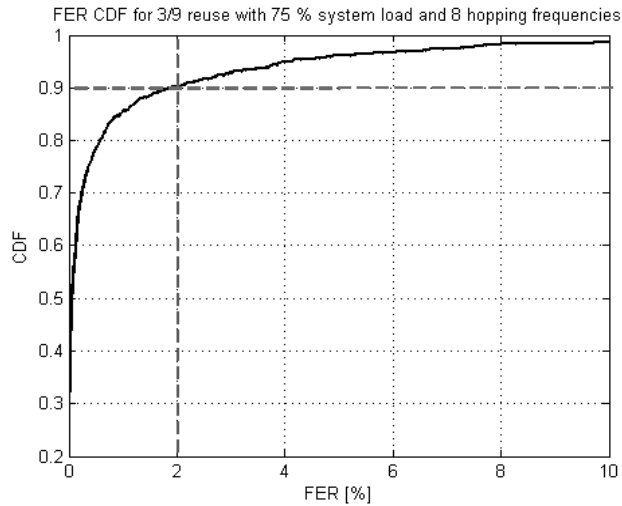


Fig 29 at a maximum system load of 75% the FER QoS criterion is satisfied at 90% of the service area

## 6. Conclusions

Various interference mitigation techniques can be deployed by the GSM network operator in order to improve its Carrier-to-Interference ratio statistics. These techniques include: Discontinuous transmission (DTX), Power Control (PC) and Frequency Hopping (FH). In DTX, the silence frames of a MS are exploited as periods of power reduction, and thus the overall interference encountered by the BTS is reduced in proportion with the Voice Activity Factor (VAF). Using Power Control (PC), the relative distance between the MS and BTS controls the amount of transmitted power. A MS that is quite close to the home BTS can transmit far less power and thus, overall network interference is reduced. Another feature of GSM is Frequency Hopping; transmission at a different RF carrier every burst reduces the probability that reuse cells' interferers collide with the home cell user by a factor that depends on the system load and number of hopping frequencies. The effect of these techniques was studied and improvements in C/I statistics were presented for a practical simulation environment that includes the antenna's radiation pattern, path loss, slow and fast fading. It was shown that capacity of a GSM network can be improved by adopting a tight reuse scheme in conjunction with DTX, PC and FH features maintaining QoS perceived by the user. This QoS is quantified in terms of FER. Spectral Capacity is a network assessment metric that relates the operator's revenues (traffic) with the investment costs (allocated spectrum and base station density). The spectral capacity of a conventional reuse scheme of 4/12 was compared to a tighter 3/9 scheme that deploys DTX, PC and FH. A boost of 25 % in spectral capacity was detected for the 3/9 scheme maintaining the soft blocking QoS criterion.

## References

- [1] Theodore S. Rappaport, "Wireless Communications: Principles and Practice", Pearson, 2<sup>nd</sup> edition, 2009, p 41.
- [2] Thomas Toftegaard Nielsen, Jeroen Wigard, "Performance Enhancements in Frequency Hopping GSM Network", Springer, 2000, pp 187 – 207.
- [3] GSM 05.02, "Wireless Multiplexing and multiple access on the radio path", ETSI, 1996.

- [4] Stefan Briick, "Modelling Interference Diversity in GSM Networks", Vehicular Technology Conference, 2000. IEEE VTS-Fall VTC 2000. 52nd, pp 459 – 466.
- [5] Hikan Olofsson, Jonas Naslund, Johan Skold, "Interference Diversity Gain in Frequency Hopping GSM", Vehicular Technology Conference, 1995 IEEE 45th, pp 102-106.
- [6] Jeroen Wigard and Preben Mogensen, "A Simple Mapping from C/I to FER and BER for a GSM Type Air-Interface", Personal, Indoor and Mobile Radio Communications, 1996. PIMRC'96. Seventh IEEE International Symposium on, pp 78 – 82.
- [7] J Pons and J Dunlop, "Enhanced system level/link level simulation interface for GSM", Vehicular Technology Conference, 1999. VTC 1999 - Fall. IEEE VTS 50th, pp 1189 – 1193.
- [8] Carlo Caini, Guido Riva, "A New Vector Quantization Technique for Performance Evaluation in Frequency Hopping Mobile Radio Systems", IEEE COMMUNICATIONS LETTERS, VOL. 4, NO. 8, AUGUST 2000, pp 252 – 254.
- [9] GSM 03.03, "Radio Network Planning Aspects", ETSI, 1996.
- [10] GSM 05.05, "Radio Transmission and Reception", ETSI, 1993.
- [11] Martin Keller, "A comprehensive simulation approach to study FH in two GSM system regarding the physical layer level and the system level", Vehicular Technology Conference, 1997, IEEE 47<sup>th</sup>, pp 1852 – 1856.

**Ahmed M. Alaa:** Post-graduate student for Master's degree in Communications and Teaching Assistant at EECE department, Cairo University.

**Hazim Tawfik:** Professor of Wireless and Mobile Communications, EECE department, Cairo University.

**How to cite this paper:** Ahmed M. Alaa, Hazim Tawfik, "Interference Mitigation Techniques for Spectral Capacity Enhancement in GSM Networks", IJWMT, vol.4, no.1, pp.20-49, 2014. DOI: 10.5815/ijwmt.2014.01.03